Title

Structural Evolution of Environmentally Responsive Cationic Liposome—DNA Complexes with a Reducible Lipid Linker

Journal

Langmuir, 28(28)

ISSN

0743-7463

Authors

Shirazi, Rahau S

Ewert, Kai K

Silva, Bruno FB

et al.

Publication Date

2012-07-17

DOI

10.1021/la301181b

Published in final edited form as:
Langmuir. 2012 July 17; 28(28): 10495–10503. doi:10.1021/la301181b.

Structural Evolution of Environmentally Responsive Cationic Liposome–DNA Complexes with a Reducible Lipid Linker

Rahau S. Shirazi[a], **Kai K. Ewert**[b], **Bruno F. B. Silva**[b,c], **Cecilia Leal**[b,d], **Youli Li**[e], and **Cyrus R. Safinya**[b,*]

[a]Department of Chemistry and Biochemistry, University of California at Santa Barbara, Santa Barbara, California 93106, United States

[b]Department of Materials, Department of Physics, and Molecular, Cellular & Developmental Biology Department, University of California at Santa Barbara, Santa Barbara, California 93106, United States

[c]Division of Physical Chemistry, Centre for Chemistry and Chemical Engineering, Lund University, SE-221 00 Lund, Sweden

[e]Materials Research Laboratory, University of California, Santa Barbara, California 93106, United States

Abstract

Environmentally responsive materials, i.e., materials that respond to changes in their environment with a change in their properties or structure, are attracting an increasing amount of interest. We recently designed and synthesized a series of cleavable multivalent lipids (CMVLn, with n = 2 to 5 the number of positive headgroup charges at full protonation) with a disulfide bond in the linker between cationic headgroup and hydrophobic tails. The self-assembled complexes of the CMVLs and DNA are a prototypical environmentally responsive material, undergoing extensive structural rearrangement when exposed to reducing agents. We investigated the structural evolution of CMVL–DNA complexes at varied complex composition, temperature and incubation time using small-angle X-ray scattering (SAXS) and wide-angle X-ray scattering (WAXS). A related lipid with a stable linker, TMVL4, was used as a control. In a nonreducing environment CMVL–DNA complexes form the lamellar (L_α^C) phase, with DNA rods sandwiched between lipid bilayers. However, new self-assembled phases form when the disulfide linker is cleaved by dithiothreitol or the biologically relevant reducing agent glutathione. The released DNA and cleaved CMVL headgroups form a “loosely organized” phase, giving rise to a characteristic broad SAXS correlation profile. CMVLs of high headgroup charge also form condensed DNA bundles. Intriguingly, the cleaved hydrophobic tails of the CMVLs reassemble into tilted chain-ordered $L_{\beta'}$ phases upon incubation at physiological temperature (37 °C), as indicated by characteristic WAXS peaks. X-ray scattering further reveals that two of the three phases ($L_{\beta F}$, $L_{\beta L}$, and $L_{\beta I}$) comprised by the $L_{\beta'}$ phase coexist in these samples. The described system may have applications in lipid-based nanotechnologies.

Cyrus R. Safinya (safinya@mrl.ucsb.edu, fax number: 805 893 8797).
[d]present address: Department of Materials Science and Engineering, University of Illinois, Urbana-Champaign, Illinois 61801, United States

SUPPORTING INFORMATION AVAILABLE
Additional SAXS data as outlined in the text. This material is available free of charge via the Internet at http://pubs.acs.org.

Keywords

Environmentally responsive materials; degradable linker; disulfide; DNA condensation

INTRODUCTION

Environmentally responsive materials are designed to switch functional properties (e.g., triggerable and controlled release of entrapped molecules and sensing nanoprobes[1]) in response to environmental stimuli (e.g., change of pH, UV irradiation, change of redox potential).[2–4] Recently, environmentally responsive materials capable of condensing DNA have received increasing attention due to their potential to improve controlled release[5–10] and reduce cell toxicity in biological environments.[11–13] In particular, materials containing reducible disulfide bonds have attracted strong interest. Disulfide bonds can be reductively cleaved into the constituting thiols, e.g., in the reducing environment of the intracellular matrix while they are stable in the extracellular space. This feature is exploited by biological systems[14,15] and increasingly in synthetic materials for a variety of biomolecular materials and biomedical applications.[16,17] Specific examples include nucleic acid delivery vectors[5–13,18,19] and imaging agents.[20,21] More broadly, environmentally responsive materials exhibiting changes in shape (shrinking or swelling), mechanical, or other properties due to changes in pH, salt concentration, or temperature are studied for a range of applications including chemical valves and actuators,[22,23] chemical sensing, and chemical encapsulation and controlled release.[24–26]

The interaction of cationic liposomes and DNA leads to the formation of cationic liposome (CL)–DNA complexes with organized self-assembled structures.[27–29] These CL–DNA complexes can be employed as nonviral vectors for DNA delivery.[30–37] CL–DNA complexes form distinct self-assembled structures,[34–37] depending mainly on the preferred curvature, or packing properties (ratio of the projected areas of headgroup and alkyl tails), of the used lipid mixture. The three main types of self-assembled structures are: (i) the most common lamellar phase (L_α^C), a multilamellar structure with DNA monolayers sandwiched between cationic membranes;[27] (ii) the inverted hexagonal phase (H_{II}^C), with DNA encapsulated within cationic lipid monolayer tubes;[29] and (iii) the hexagonal phase (H_I^C), comprising hexagonally arranged rod-like lipid micelles that are surrounded by DNA chains forming a substructure with honeycomb symmetry.[38]

Previously, we have synthesized a series of cleavable multivalent lipids, (CMVLs)[11], with charges from +2 *e* to +5 *e* and a disulfide linker connecting the cationic headgroup to the aliphatic tails. Preliminary SAXS studies showed that DNA complexes of mixtures of the CMVLs with varied amounts of the neutral lipid (NL) 1,2-dioleoyl-*sn-glycero*-3-phosphatidylcholine (DOPC) formed the lamellar phase (L_α^C), and that reductive cleavage of the disulfide linker by reducing agents disassembled the complexes.[11]

In this work, we present a detailed study of the structural evolution of CMVL–DNA complexes in response to stimuli such as a reducing environment (i.e., chemical sensing) and temperature. Disassembly of a lamellar phase is followed by a remarkable reassembly into new structures. We used synchrotron SAXS and WAXS to study the DNA complexes of CMVLs mixed with DOPC as a function of lipid composition, cationic to anionic charge ratio (ρ), temperature, and time. As a control we also investigated TMVL4 (4+), an analogue of CMVL4 with a spacer that is stable to the employed reducing agents. We used two different reducing agents: the strong reducing agent dithiothreitol (DTT) and the biologically relevant reducing agent Glutathione (L-γ-glutamyl-L-cysteinylglycine, GSH). GSH is the most abundant thiol-source in mammalian cells, at up to millimolar concentrations.[39]

Exposure to a reducing environment cleaves the disulfide linker of the CMVLs, and the head group detaches from the lipid tail. Consequently, the initial lamellar (L_α^C) phase of the complexes disassembles. This releases the cationic headgroups which then form new self-assembled phases with the anionic DNA. The headgroups (2+ to 5+) condense the released DNA into a disordered ("loosely organized") phase with a characteristic broad SAXS correlation profile. CMVLs with high headgroup charge can further condense the DNA into hexagonal bundles. This behavior of the headgroups is similar to that of cationic surfactant micelles in cationic surfactant-polyelectrolyte mixtures. Recent SAXS studies have shown that such mixtures form concentrated phases that can evolve from a cubic to a hexagonal and then lamellar phase.[40,41] The cleaved hydrophobic tails of the CMVLs form separate self-assembled structures. SAXS shows that triggered by incubation at 37 °C, they reassemble from a highly disordered lamellar phase into a chain-ordered and tilted $L_{\beta'}$ phase in which two of the three chain-ordered lamellar phases ($L_{\beta F}$, $L_{\beta L}$, and $L_{\beta I}$) comprised by the $L_{\beta'}$ phase coexist.[42–44]

EXPERIMENTAL SECTION

Materials

DOPC was purchased from Avanti Polar Lipids. The CMVLs were synthesized as previously described.[11] TMVL4 was synthesized as described for TMVL5,[45] using Boc-protected carboxyspermine[38,46] as the headgroup building block. Opti-MEM cell culture medium (a modified Dulbecco's modified Eagle's medium, containing approximately 150 mM monovalent salt and 99.9 mg/L $CaCl_2$, buffered at pH =7.4) was purchased from Invitrogen. Highly polymerized calf thymus (HPCT) DNA (average molecular weight 10000–15000 kDa) was purchased from Sigma-Aldrich. Other chemicals were purchased from Fisher Scientific unless otherwise stated, and were used as received.

Lipid suspensions

Lipid stock solutions were prepared in chloroform/methanol (9:1, v/v; for TMVL4 and all CMVLs) or chloroform (DOPC) and combined at the appropriate ratios in glass vials. The resulting lipid solutions were dried, first using a stream of nitrogen and then by incubation in a vacuum for 12 h, forming a thin lipid film. The lipid film was hydrated using sterile high resistivity (18.2 MΩ cm) water, incubating at 37 °C for at least 12 h to produce suspensions of a final concentration of 50 mM. The aqueous lipid suspensions were tip-sonicated to clarity (Vibra-cell, Sonics Materials) and stored at 4 °C until use.

Small-angle X-ray Scattering

High-resolution SAXS experiments were performed at the Stanford Synchrotron Radiation Lightsource. The X-ray samples were prepared from 50 mM lipid suspensions and 4 mg/mL DNA stock solutions, using a constant 100 μg of DNA per sample. The amount of CMVL was varied according to the desired cationic to anionic charge ratio, ρ, assuming the headgroups of the CMVLs to be fully protonated. We calculated this charge ratio as $\rho = N+/N- = n\,N_{CMVLn}/N_{nt}$. Here, $N+$ and $N-$ are the numbers of positive (lipid) and negative (DNA) charges, respectively, and N_{CMVLn} and N_{nt} are the amounts (in mol) of CMVLn (with n the valence of CMVLn) and nucleotides (bearing one negative charge each) in the sample, respectively. CL–DNA complexes were formed by combining CL and DNA solutions in microcentrifuge tubes and diluting with an equal volume of Opti-MEM. Thus, the final medium (after mixing) for all samples was a 1:1 (v:v) mixture of water and Opti-MEM. Extensive centrifugation yielded the CL–DNA complexes as an opaque white precipitate. The CL–DNA complexes containing reducing agents were prepared at least two hours prior to the addition of reducing agent. DTT and GSH stock solutions in a 1:1 (v:v) mixture of sterile high resistivity (18.2 MΩ cm) water and Opti-MEM were freshly prepared

at 300 mM. The mole ratio of reducing agent thiol groups to lipid was ≥ 60, and an equal number of thiol groups was added for each reducing agent (GSH contains one thiol group, while DTT contains two). All samples were prepared and measured at room temperature. Samples without reducing agent were incubated at 4 °C for at least three days following preparation (before measurements, in order to reach equilibrium) unless otherwise stated. The other samples were also stored at 4 °C between preparation and measurement except for the specified incubation times at higher temperature. SAXS measurements were performed at multiple positions throughout the opaque precipitate (pellet) as well as the supernatant, and representative scans are shown for all samples.

RESULTS AND DISCUSSION

CL–DNA complexes of reductively cleavable CMVLs are an environmentally responsive biomaterial, undergoing large structural changes in response to an external stimulus (redox potential in solution). The basis of this is the design of the CMVLs. Figure 1A shows their chemical structures as well as those of the neutral lipid DOPC and of TMVL4, an analogue of CMVL4 that is stable to the employed reducing conditions. Figure 1B shows molecular models of these lipids. The cationic headgroups of the CMVLs and TMVL4 are attached to the hydrocarbon tails via a short linker. This linker is derived from disulfide bond-containing cystamine in the case of the CMVLs and from a short PEG unit in the case of TMVL4. Red arrows in Figure 1A point to the disulfide bonds, which are cleaved into the two constituting thiols in a reducing environment. The amphiphilicity of the CMVLs is tied to the integrity of the linker because of its position within the molecule (connecting the hydrophobic and hydrophilic parts). Consequently, a change in environments that will affect the stability of the linker will control the stability of self-assembled phases formed by the CMVLs.

To investigate the structural evolution of CMVL-based CL–DNA complexes in detail, we performed X-ray diffractions studies as a function of CMVL valence (2+ to 5+), temperature, time, and compositional variables of the complexes. The key compositional parameters of CMVL-based CL–DNA complexes are the cationic (CMVL) to anionic (DNA) charge ratio, ρ, and the lipid composition (the ratio of CMVL to DOPC, which determines the charge density of the membranes) given by the mol fraction of CMVL in the membrane, $\Phi_{CMVL} = 1 - \Phi_{DOPC}$. We employed two different reducing agents: dithiothreitol (DTT), a strong reducing agent used routinely in chemical biology to cleave disulfide bonds and the biologically relevant reducing agent glutathione (L-γ-glutamyl-L-cysteinylglycine, GSH), which is the most abundant thiol source in mammalian cells, at up to millimolar concentrations.[39]

Figure 2 summarizes our results. Cationic liposomes (CLs) prepared from mixtures of a cationic CMVL and neutral DOPC form complexes with negatively charged DNA (Figure 2a). Depending on the charge ratio (ρ), the resulting complexes are anionic, neutral or cationic (Figure 2, parts b–d). In a reducing environment the disulfide linker of the CMVLs is cleaved, separating the cationic headgroup from the hydrophobic tail. This leads to disassembly of the lamellar complex phase ($L_\alpha{}^C$)[11] (Figure 2e) and formation of new self-assembled structures. X-ray diffraction shows that self-assembly of the cleaved tails into a chain-ordered and tilted phase can be triggered by temperature (37 °C) (Figure 2f). The released DNA and CMVL headgroups form a “loosely organized” phase with a characteristic broad SAXS correlation profile (Figure 2g). In some cases, this organization evolves into a more ordered phase, as observed in particular for the highly charged CMVL5 (5+) (Figure 2h).

Structural Characterization of CMVL–DNA Complexes in Nonreducing Media

CMVL/DOPC–DNA complexes form the lamellar phase in the absence of reducing agents for all compositions investigated. Figure 3 illustrates this, using CMVL4/DOPC–DNA complexes as an example (cf. the Supporting Information for representative SAXS data confirming the lamellar structure for DNA complexes of the other CMVLs). Figure 3A shows SAXS patterns for CMVL4/DOPC–DNA complexes at $\rho = 4$ and several Φ_{CMVL4}. These complexes had been stored at 4 °C after preparation. As highlighted by arrows for $\Phi_{CMVL} = 0.8$, the lamellar ordering gives rise to a series of sharp peaks labeled q_{001}, q_{002}, q_{003}, and q_{004}, corresponding to a lamellar repeat distance of $d = 2\pi/q_{001} = 2\pi/0.084$ Å^{-1} = 74.8 Å. The one-dimensional smectic order of the DNA molecules within the lamellar complex gives rise to the peak at q_{DNA}, which allows calculation of the interhelical spacing as $d_{DNA} = 2\pi/q_{DNA} = 26.7$ Å.[27,45,47] The DNA–DNA correlation peak is broader and weaker than the peaks arising from the lamellar ordering and frequently overlaps with them.[48,49] Nonetheless, its characteristic shift to lower q (larger d_{DNA}, less condensed DNA) with decreasing Φ_{CMVL4} is evident. For $\Phi_{CMVL4} = 0.6$, $d_{DNA} = 29.9$ Å and for $\Phi_{CMVL4} = 0.4$, $d_{DNA} = 31.4$ Å. The characteristic SAXS pattern of the $L_\alpha{}^C$ phase is present over the whole range of Φ_{CMVL4}, even as the peaks characteristically broaden[45] at high content of CMVL4 ($\Phi_{CMVL4} = 1$). The data in Figure 3B illustrates that the lamellar phase also prevails at lower ρ ($\rho = 1, 3$), as shown for $\Phi_{CMVL4} = 0.6$. This Φ_{CMVL} marks the optimum performance CMVL4/DOPC–DNA complexes in DNA transfection assays.[11,45] SAXS profiles for the complete range of Φ_{CMVL4} for $\rho = 1$ and 3 are shown in the Supporting Information (Figure S1).

Figure 4 compares the time evolution of the SAXS profiles of DNA complexes of CMVL4 and TMVL4, the stable analogue of CMVL4, in the absence of reducing agents (for $\rho = 4$, $\Phi_{MVL} = 0.6$). The samples were stored for three months at 4 °C after preparation, measured (red curves), stored for another 3 months at room temperature, and measured again (black curves). All SAXS scans exhibit the typical pattern of the lamellar phase, indicating that the lamellar DNA complexes formed from the CMVLs are stable for at least six months after preparation and demonstrating the stability of the disulfide linker in cell culture medium in the absence of reducing agent (complexes were prepared in a 1:1 (v:v) mixture of water and Opti-MEM, a cell culture medium).

Structure Evolution of CMVL–DNA Complexes in a Reducing Environment

To create a reducing environment, we added a solution of reducing agent to the complexes, in some cases varying also the incubation temperature. DTT is a strong reducing agent which reliably cleaves disulfide bonds but not necessarily reproduces the reducing environment inside the cell. In contrast, the milder agent GSH is an important biological reducing agent, present in considerable amounts in animal cells.[39] Thus, DTT served as a reference agent to ensure that CMVL cleavage occurs, while GSH more closely resembled biologically relevant conditions.

The addition of reducing agent has no effect on the DNA complexes of TMVL4, the stable analog of CMVL4. The SAXS data displayed in Figure 5A shows that the lamellar phase of TMVL4/DOPC–DNA complexes ($\rho = 4$, $\Phi_{TMVL4} = 0.6$) for both standard sample treatment (incubation at 4 °C) and incubation for 8 h at 37 °C, with and without DTT or GSH. In contrast, the addition of reducing agent disassembles the lamellar phase of CMVL4/DOPC–DNA complexes, i.e., the characteristic q_{00L} and q_{DNA} peaks disappear. The data in Figure 5B shows (for complexes at $\rho = 4$ and $\Phi_{CMVL4} = 0.6$) that a trace of lamellar phase remains (as indicated by a residual q_{001} peak) only when GSH is used as the reducing agent. The main new feature in the SAXS scans of CMVL4-containing complexes after addition of reducing agent is a broad peak at $q = 0.12$ to 0.15 Å^{-1}, corresponding to a real space

periodicity of d = 41 to 52 Å ($2\pi/q$). Since the only difference between TMVL4 and CMVL4 is in the spacer, this data confirms our design strategy of introducing a disulfide bond in order to generate an material undergoing structural change in response to the environment (in this case the redox potential). Further confirmation comes from the fact that similar behavior (a broad peak replacing the lamellar peaks) is also observed for CMVL5,[11] CMVL3, and CMVL2 (cf. Figures S2 to S5 in the Supporting Information and Figure 6A). In the case of CMVL5 an additional, sharper peak is observed at around $q = 0.24$ Å^{-1} as shown in Figure 6A. A trace of a similar peak is visible also for CMVL4/DOPC–DNA complexes treated with DTT (Figure 5B). Hexagonal bundling of DNA by small multivalent counterions gives rise to a SAXS peak of similar width and position.[50] Formation of such condensed DNA bundles in bulk requires counterions with valence ≥ 3.[51–54] The reason that only the headgroups of CMVL5 tightly bundle DNA to a significant extent in our system may be that the CMVL headgroups are not fully protonated in neutral aqueous solution. The cleaved CMVL headgroups are also significantly larger than inorganic counterions, i.e., their charge density is smaller, which may reduce their ability to condense DNA into tight bundles.

The broad peak at low q (0.12 to 0.15 Å^{-1}), corresponding to a real space correlation length ($2\pi/q$) of 41 to 52 Å may result from scattering by a highly disordered (defect-rich) lamellar phase with bilayers consisting of the cleaved CMVL tails (with slightly a polar amide and SH headgroup) and DOPC. This is a kinetically trapped intermediate structure on a temperature-dependent pathway, which ultimately leads to a lower energy phase consisting of highly ordered and tilted lipid chains (see below). Another possible source of the observed broad peak is scattering from a loosely condensed phase formed by the cleaved multivalent headgroups and DNA (cf. Figure 2g). The SAXS peak of such a phase (which coexists with a phase of tight bundles for CMVL4 and CMVL5) is expected to be broad because the mesh size is highly polydisperse. In fact, both phases are present and their peaks overlap: for several samples at high Φ_{CMVL} (where the bilayer-derived peak is smaller) two separate broad peaks are resolved in the SAXS patterns (cf. Figure S6 in the Supporting Information). At lower Φ_{CMVL}, the broader peak due to the disordered lamellar phase dominates.

Elevated temperature accelerates the structural changes induced by reducing agents. For example, replacement of the lamellar SAXS pattern with the broad peak at 0.13 Å^{-1} took days at 4 °C, but only 8 hours at 37 °C (cf. Figure 5). This is likely due to enhanced diffusion of GSH into the bilayer-based liquid crystalline structure at 37 °C. The fact that an increase in the mole fraction of the DOPC (Φ_{DOPC}) in the complexes drastically reduces the rate of the reduction reaction further highlights the importance of diffusion of reducing agent into the complexes, which have been compacted into a condensed pellet during sample preparation. Isoelectric and negatively charged complexes ($\rho = 1$ and $\rho = 0.5$, respectively) also show the broad peak at $q \approx 0.13$ Å^{-1} after treatment with GSH and incubation at 37 °C (Figure S7 in the Supporting Information). No residual scattering from a lamellar phase is seen for these samples.

Recent SAXS studies on analogous cationic surfactant-polyelectrolyte systems have shown that such mixtures can form concentrated phases that can evolve from a cubic to hexagonal and then lamellar phase.[40] For the charged particles with poly-counterions containing at least three ionic units, the spherical micelles can aggregate. On the other hand, an increase in the number of uncharged units decreases the surfactant aggregate and such an increase can eventually destroy the ordered liquid crystalline assembly.[41] We hypothesize that, to a certain extent, the headgroups resulting from cleavage (headgroups of +2 to +5 charge) behave similarly to the cationic surfactant micelles, and therefore will also bundle and condense the DNA into close-packed disordered structures that under some conditions (e.g.,

sufficiently large headgroup charge) can nucleate into more ordered liquid crystalline structures.

Structures Formed by the Cleaved Hydrocarbon Tails at Physiological Temperature

Cleavage of the linker of the CMVLs in a reducing environment also releases the hydrophobic tails, which together with DOPC initially form a disordered, defect-rich lamellar phase (see above). Annealing this phase at physiological temperature activates a reassembly of the lipid tails, as we show below.

Several lamellar lipid phases exist, distinguished by the degree of ordering of the hydrophobic tails. These include the chain-melted L_α phase, and the chain-ordered L_β and $L_{\beta'}$ phases.[42–44] Transitions between these phases can occur as a function of temperature, water content, and nature of the lipid.[42,44,55–58] Reducing the water content of a lamellar phase can induce the transition from the L_α to the $L_{\beta'}$ and further to the L_β phase with increasing dehydration. X-ray diffraction is well suited to distinguish between the different phases.[42,43] The order of the hydrocarbon chains in the L_α phase is liquid-like with no regular in-plane structure. In contrast, the chains are extended and tightly packed in a two-dimensional, quasi-hexagonal lattice in the L_β and $L_{\beta'}$ phases. In the L_β phase, the hydrocarbon chains are oriented at a right angle to the plane of the lamellae, while they are tilted in the $L_{\beta'}$ phases.[42,57] Comprehensive X-ray scattering studies of oriented, freely suspended lipid–water multilayer films by Smith et al. distinguished three distinct two-dimensional phases for the phase: $L_{\beta F}$, $L_{\beta I}$, and $L_{\beta L}$.[42–44] These differ in the direction of in-plane chain tilt with respect to their nearest neighbor (there are no in-plane correlations between bilayers), as illustrated in Figure 7. The molecules in the $L_{\beta F}$ and $L_{\beta I}$ phases are tilted in between and toward nearest neighbors, respectively. In the $L_{\beta L}$ phase, the tilt direction of the molecules is somewhere between these two extremes (Figure 7b).[42–44] For DMPC (1,2-dimyristoyl-*sn*-glycero-3-phosphatidylcholine), these $L_{\beta'}$ phases shows peaks at $q = 1.350$ and 1.446 $Å^{-1}$ ($L_{\beta F}$), $q = 1.365$ and 1.475 $Å^{-1}$($L_{\beta I}$), and $q = 1.355$, 1.399, and 1.468 $Å^{-1}$($L_{\beta L}$).[42]

In the lamellar CMVL–DNA complexes as well as after addition of reducing agent at room temperature and prolonged storage of the same sample at lower temperature (4 °C), the lipid tails are in the chain-melted state. Figure 6A illustrates this by showing the X-ray scattering patterns of CMVL5/DOPC–DNA complexes at $\Phi_{CMVL5} = 0.6$ and $\rho = 3$. In the absence of reducing agent (black curve, top), the characteristic peaks of the lamellar $L_\alpha{}^C$ phase are observed (black arrows; $q_{001} = 0.0825$ $Å^{-1}$), with a DNA–DNA spacing of $d_{DNA} = 27.3$ Å (red arrow marks q_{DNA}). After addition of DTT at room temperature (red curve), these peaks disappear, and instead a sharp peak at $q = 0.26$ $Å^{-1}$ (DNA bundles) as well as a broad peak at $q \approx 0.13$ $Å^{-1}$ (bilayers and loosely organized DNA–headgroup phase) are visible. A similar (same composition, prepared independently) sample shows a sharp peak at $q = 0.24$ $Å^{-1}$ and a broad peak at $q \approx 0.13$ $Å^{-1}$ (blue curve; peak assignment as above) after 48 months incubation at 4 °C. The scattering background from a sample containing only the medium in which the complexes were prepared (water:Opti-MEM, 1:1, v:v) is also shown (gray curve). The very broad peak between $q = 1.3$ to 1.7 $Å^{-1}$, visible for all samples, is the characteristic correlation peak of the disordered hydrophobic tails.

Incubation at 37 °C triggers a reassembly of the hydrophobic chains. Figure 6B shows scattering patterns of CMVL5/DOPC–DNA complexes ($\rho = 3$; $\Phi_{CMVL5} = 0.4$, 0.6, and 0.7) that were incubated for 24 h at 37 °C after addition of DTT. For $\Phi_{CMVL5} = 0.7$, two new series of peaks indexing to a lamellar structure can be identified, where $q_{001} = 0.12$ $Å^{-1}$ and $q_{001} = 0.13$ $Å^{-1}$ (with 6 and 3 orders of diffraction peaks visible, respectively). Furthermore, distinct new peaks at wide angles ($q = 1.45$ $Å^{-1}$, $q = 1.46$ $Å^{-1}$, $q = 1.48$ $Å^{-1}$, and $q = 1.51$ $Å^{-1}$) indicate that the newly formed lamellar structures are chain-ordered phases. Figure 6B

shows that similar patterns were observed for $\Phi_{CMVL5} = 0.6$ and $\Phi_{CMVL5} = 0.4$. Likely, two of the three phases ($L_{\beta F}$, $L_{\beta L}$, and $L_{\beta I}$) which the $L_{\beta'}$ phase comprises[42] coexist in these samples.

The fact that increased temperature triggers the transition to the more ordered $L_{\beta'}$ phase may initially appear counterintuitive because the chain-ordered phases exist at lower temperatures than the chain-melted L_α phase for a given lipid. However, in our system, the lipid tails stay the same but addition of the reducing agent strongly alters the headgroups. The comparatively large, highly hydrophilic and charged (and thus well-hydrated) headgroups of the CMVLs are cleaved off and only the thiol group and other parts of the spacer remain as the polar part of the molecule. This conversion to a smaller headgroup and the concomitant dehydration favor denser packing of the hydrophobic tails, which in turn promotes formation of chain-ordered phases. This has been well documented in particular for the dehydration of lipid lamellar phases.[42] Incubation at 37 °C likely promotes formation of the $L_{\beta'}$ phase by annealing the many defects present in the structure formed by the CMVL tails and DOPC upon CMVL cleavage (the fact that the corresponding SAXS peak is very broad confirms the high defect density, see above). At 4 °C, the disordered phase is kinetically trapped and the $L_{\beta'}$ phases are not observed.

Interestingly, $L_{\beta'}$ phases form with DTT as the reducing agent, but not with GSH in otherwise identical conditions. Incubation of CMVL5/DOPC–DNA complexes ($\rho = 3$; $\Phi_{CMVL5} = 0.6$) at 37 °C with GSH disassembles the $L_\alpha{}^C$ phase as indicated by the disappearance of the corresponding (00L) diffraction peaks, but no $L_{\beta'}$ phase is observed even after an additional 24 hours of incubation at 37 °C (cf. Figure S5 in the Supporting Information). Possibly, the oxidized form of the reducing agent (the byproduct of the cleavage reaction) interferes with the formation of the $L_{\beta'}$ phase. The oxidized form of DTT is a small cyclic molecule, while the oxidized form of GSH (GSSG; two tripeptides linked by a disulfide bond) is bulky and hydrophilic. In addition, intramolecular cyclization of DTT in the process of reducing a disulfide bond (the reason for its high efficiency as a disulfide reducing agent) ensures that mixed disulfide intermediates of the reaction do not accumulate. This may be different for GSH, which could form GS-S-tail intermediates, which essentially are lipids with a relatively large (and presumable well-hydrated) headgroup that are not prone to formation of the dehydrated $L_{\beta'}$ phase.

CONCLUSIONS

Using X-ray diffraction, we have studied environmentally responsive CL–DNA complexes prepared from mixtures of DOPC and a series of CMVLs (2+ to 5+) as well as TMVL4 (4+, a stable analog of CMVL4). In the absence of reducing agents, all these lipids form lamellar ($L_\alpha{}^C$) complexes with DNA. Incubation of CMVL-based complexes in a reducing environment cleaves the disulfide linker between CMVL headgroup and tail, and new self-assembled phases form at the expense of the $L_\alpha{}^C$ phase. The released DNA and CMVL headgroups form a “loosely organized” phase as well as tight DNA bundles for highly charged CMVLs. The cleaved hydrophobic tails of the CMVLs and DOPC form a disordered lamellar phase which reassembles into chain-ordered lamellar structures after incubation at physiological temperature. WAXS reveals coexistence of two of the three chain-ordered and tilted lamellar phases ($L_{\beta F}$, $L_{\beta L}$, and $L_{\beta I}$) comprised by the $L_{\beta'}$ phase.

Lamellar lipid bilayer phases are ideal systems to confine biological (including DNA,[27,59] RNA,[60] peptides and proteins[61]) and synthetic (e.g., carbon nanotubes[62]) macromolecules in 2D. As described in this work, CMVL-based membranes add the element of responsiveness to such lamellar assemblies, e.g. allowing disassembly of a templating lamellar phase on demand. Due to the fact that reducing conditions (which are not limited to the thiol-

containing reducing agents employed in this work) free thiol groups from the CMVLs, they may further find uses in scientific and technological areas where shifts in environmental conditions are used to prepare self-assembled monolayers (SAMs)[63] and multilayers on gold surfaces.[64]

Supplementary Material

Refer to Web version on PubMed Central for supplementary material.

Acknowledgments

This work was supported by DOE-Basic Energy Sciences grant number DOE-DE-FG02-06ER46314 (environmentally responsive materials; dynamic evolution of self-assemblies) and the U.S. National Science Foundation DMR-1101900 (chain-ordered lipid phase behavior). We also acknowledge support by NIH GM-59288 (development of strategies for synthesis of degradable cationic lipids). Parts of the sample characterization was performed using the Central Facilities of the Materials Research Laboratory at UCSB which are supported by the MRSEC Program of the NSF under award no. DMR-1121053; a member of the NSF-funded Materials Research Facilities Network (www.mrfn.org). Cecilia Leal was funded by the Swedish Research Council (VR) and in part by the US DOE-BES. Bruno Silva was supported by a Marie Curie International Outgoing Fellowship within the EU Seventh Framework Programme for Research and Technological Development (2007–2013), project No. 252701. The X-ray diffraction work was carried out at the Stanford Synchrotron Radiation Lightsource (SSRL), a DOE National laboratory, on beam line 4.2. CRS also acknowledges useful discussions with KAIST Faculty where he has a WCU (World Class University) Visiting Professor of Physics appointment supported by the National Research Foundation of Korea funded by the Ministry of Education, Science and Technology No. R33-2008-000-10163-0.

References

1. Almutairi A, Guillaudeu SJ, Berezin MY, Achilefu S, Fréchet JM. Biodegradable pH-sensing dendritic nanoprobes for near-infrared fluorescence lifetime and intensity imaging. J Am Chem Soc. 2008; 130:444–445. [PubMed: 18088125]
2. Wang YC, Wang F, Sun TM, Wang J. Redox-responsive nanoparticles from the single disulfide bond-bridged block copolymer as drug carriers for overcoming multidrug resistance in cancer cells. Bioconjugate Chem. 2011; 22:1939–1945.
3. Zhao M, Biswas A, Hu B, Joo KI, Wang P, Gu Z, Tang Y. Redox-responsive nanocapsules for intracellular protein delivery. Biomaterials. 2011; 32:5223–5230. [PubMed: 21514660]
4. Löwik DW, Leunissen EH, van den Heuvel M, Hansen MB, van Hest JC. Stimulus-responsive peptide-based materials. Chem Soc Rev. 2010; 39:3394–3412. [PubMed: 20523948]
5. Obika S, Yu W, Shimoyama A, Uneda T, Miyashita K, Doi T, Imanishi T. A symmetrical and biodegradable cationic lipid. Synthesis and application for efficient gene transfection. Bioorg Med Chem Lett. 1997; 7:1817–1820.
6. Sheng R, Luo T, Zhu Y, Li H, Sun J, Chen S, Sun W, Cao A. The intracellular plasmid DNA localization of cationic reducible cholesterol-disulfide lipids. Biomaterials. 2011; 32:3507–3519. [PubMed: 21329973]
7. Lee Y, Mo H, Koo H, Park J, Cho M, Jin G, Park J. Visualization of the degradation of a disulfide polymer, linear poly(ethylenimine sulfide), for gene delivery. Bioconjugate Chem. 2007; 18:13–18.
8. Wang Y, Ke CY, Weijie Beh C, Liu SQ, Goh SH, Yang YY. The self-assembly of biodegradable cationic polymer micelles as vectors for gene transfection. Biomaterials. 2007; 28:5358–5368. [PubMed: 17764736]
9. Xia W, Wang P, Lin C, Li Z, Gao X, Wang G, Zhao X. Bioreducible polyethylenimine-delivered siRNA targeting human telomerase reverse transcriptase inhibits HepG2 cell growth in vitro and in vivo. J Controlled Release. 2011; 157:427–436.
10. Saeed AO, Magnusson JP, Moradi E, Soliman M, Wang W, Stolnik S, Thurecht KJ, Howdle SM, Alexander C. Modular construction of multifunctional bioresponsive cell-targeted nanoparticles for gene delivery. Bioconjugate Chem. 2011; 22:156–168.

11. Shirazi RS, Ewert KK, Leal C, Majzoub RN, Bouxsein NF, Safinya CR. Synthesis and characterization of degradable multivalent cationic lipids with disulfide-bond spacers for gene delivery. Biochim Biophys Acta. 2011; 1808:2156–2166. [PubMed: 21640069]
12. Manickam DS, Oupický D. Multiblock reducible copolypeptides containing histidine-rich and nuclear localization sequences for gene delivery. Bioconjugate Chem. 2006; 17:1395–1403.
13. Brumbach JH, Lin C, Yockman J, Kim WJ, Blevins KS, Engbersen JF, Feijen J, Kim SW. Mixtures of poly(triethylenetetramine/cystamine bisacrylamide) and poly(triethylenetetramine/cystamine bisacrylamide)-g-poly(ethylene glycol) for improved gene delivery. Bioconjugate Chem. 2010; 21:1753–1761.
14. Castellani OF, Martínez EN, Añón MC. Role of disulfide bonds upon the structural stability of an amaranth globulin. J Agric Food Chem. 1999; 47:3001–3008. [PubMed: 10552600]
15. Falnes P, Sandvig K. Penetration of protein toxins into cells. Curr Opin Cell Biol. 2000; 12:407–413. [PubMed: 10873820]
16. Meng F, Hennink W, Zhong Z. Reduction-sensitive polymers and bioconjugates for biomedical applications. Biomaterials. 2009; 30:2180–2198. [PubMed: 19200596]
17. Saito G, Swanson JA, Lee KD. Drug delivery strategy utilizing conjugation via reversible disulfide linkages: role and site of cellular reducing activities. Adv Drug Delivery Rev. 2003; 55:199–215.
18. Byk G, Wetzer B, Frederic M, Dubertret C, Pitard B, Jaslin G, Scherman D. Reduction-sensitive lipopolyamines as a novel nonviral gene delivery system for modulated release of DNA with improved transgene expression. J Med Chem. 2000; 43:4377–4387. [PubMed: 11087563]
19. Christensen LV, Chang CW, Kim WJ, Kim SW, Zhong Z, Lin C, Engbersen JF, Feijen J. Reducible poly(amido ethylenimine)s designed for triggered intracellular gene delivery. Bioconjugate Chem. 2006; 17:1233–1240.
20. Ke T, Feng Y, Guo J, Parker D, Lu Z. Biodegradable cystamine spacer facilitates the clearance of Gd(III) chelates in poly(glutamic acid) Gd-DO3A conjugates for contrast-enhanced MR imaging. Magn Reson Imaging. 2006; 24:931–940. [PubMed: 16916710]
21. Lu Z, Wang X, Parker D, Goodrich K, Buswell H. Poly(L-glutamic acid) Gd(III)-DOTA conjugate with a degradable spacer for magnetic resonance imaging. Bioconjugate Chem. 2003; 14:715–719.
22. Derossi, D.; Kajiwara, K.; Osada, Y.; Yamauchi, A. Polymer gels: Fundamentals and biomedical applications. Plenum Publishing; New York: 1991.
23. Osada Y, Ross-Murphy SB. Intelligent Gels. Sci Am. 1993; 268:82–87.
24. Hoffman AS. Applications of thermally reversible polymers and hydrogels in therapeutics and diagnostics. J Controlled Release. 1987; 6:297–305.
25. Peppas NA, Langer R. New challenges in biomaterials. Science. 1994; 263:1715–1720. [PubMed: 8134835]
26. Mart RJ, Osbourne RD, Stevens MM, Ulijn RV. Peptide-based stimuli-responsive biomaterials. Soft Matter. 2006; 2:822–835.
27. Rädler J, Koltover I, Salditt T, Safinya C. Structure of DNA-cationic liposome complexes: DNA intercalation in multilamellar membranes in distinct interhelical packing regimes. Science. 1997; 275:810–814. [PubMed: 9012343]
28. Lasic DD, Strey H, Stuart MCA, Podgornik R, Frederik PM. The Structure of DNA-Liposome Complexes. J Am Chem Soc. 1997; 119:832–833.
29. Koltover I, Salditt T, Rädler J, Safinya C. An inverted hexagonal phase of cationic liposome-DNA complexes related to DNA release and delivery. Science. 1998; 281:78–81. [PubMed: 9651248]
30. Felgner PL, Gadek TR, Holm M, Roman R, Chan HW, Wenz M, Northrop JP, Ringold GM, Danielsen M. Lipofection: a highly efficient, lipid-mediated DNA-transfection procedure. Proc Natl Acad Sci U S A. 1987; 84:7413–7417. [PubMed: 2823261]
31. Huang, L.; Hung, M-C.; Wagner, E., editors. Advances in Genetics. 2. Vol. 53. Elsevier; San Diego: 2005. Non-Viral Vectors for Gene Therapy.
32. Chesnoy S, Huang L. Structure and function of lipid-DNA complexes for gene delivery. Annu Rev Biophys Biomol Struct. 2000; 29:27–47. [PubMed: 10940242]
33. Niidome T, Huang L. Gene therapy progress and prospects: nonviral vectors. Gene Ther. 2002; 9:1647–1652. [PubMed: 12457277]

34. Ewert K, Slack NL, Ahmad A, Evans HM, Lin AJ, Samuel CE, Safinya CR. Cationic lipid-DNA complexes for gene therapy: understanding the relationship between complex structure and gene delivery pathways at the molecular level. Curr Med Chem. 2004; 11:133–149. [PubMed: 14754413]
35. Ewert, K.; Evans, HM.; Ahmad, A.; Slack, NL.; Lin, AJ.; Martin-Herranz, A.; Safinya, CR. Lipoplex Structures and Their Distinct Cellular Pathways. In: Huang, L.; Hung, M-C.; Wagner, E., editors. Non-viral Vectors for Gene Therapy. 2. Vol. 53. Elsevier; San Diego: 2005. p. 119-155.Advances in Genetics
36. Ewert KK, Ahmad A, Evans HM, Safinya CR. Cationic lipid-DNA complexes for non-viral gene therapy: Relating supramolecular structures to cellular pathways. Expert Opin Biol Ther. 2005; 5:33–53. [PubMed: 15709908]
37. Ewert KK, Zidovska A, Ahmad A, Bouxsein NF, Evans HM, McAllister CS, Samuel CE, Safinya CR. Cationic Liposome–Nucleic Acid Complexes for Gene Delivery and Silencing: Pathways and Mechanisms for Plasmid DNA and siRNA. Top Curr Chem. 2010; 296:191–226. [PubMed: 21504103]
38. Ewert K, Evans H, Zidovska A, Bouxsein N, Ahmad A, Safinya C. A columnar phase of dendritic lipid-based cationic liposome-DNA complexes for gene delivery: hexagonally ordered cylindrical micelles embedded in a DNA honeycomb lattice. J Am Chem Soc. 2006; 128:3998–4006. [PubMed: 16551108]
39. Meister A, Anderson M. Glutathione. Annu Rev Biochem. 1983; 52:711–760. [PubMed: 6137189]
40. dos Santos S, Lundberg D, Piculell L. Responsive and evolving mixtures of a hydrolyzing cationic surfactant and oppositely charged polyelectrolytes. Soft Matter. 2011; 7:5540–5544.
41. Piculell L, Norrman J, Svensson A, Lynch I, Bernardes J, Loh W. Ionic surfactants with polymeric counterions. Adv Colloid Interface Sci. 2009; 147:228–236. [PubMed: 18977468]
42. Smith G, Sirota E, Safinya C, Clark N. Structure of the L beta phases in a hydrated phosphatidylcholine multimembrane. Phys Rev Lett. 1988; 60:813–816. [PubMed: 10038659]
43. Smith GS, Safinya CR, Roux D, Clark NA. X-ray Study of Freely Suspended Films of a Multilamellar Lipid System. Mol Cryst Liq Cryst. 1987; 144:235–255.
44. Smith GS, Sirota EB, Safinya CR, Plano RJ, Clark NA. X-ray Structural Studies of Freely Suspended Hydrated DMPC Multimembrane Films. J Chem Phys. 1990; 92:4519–4529.
45. Ahmad A, Evans HM, Ewert K, George CX, Samuel CE, Safinya CR. New multivalent cationic lipids reveal bell curve for transfection efficiency versus membrane charge density: lipid-DNA complexes for gene delivery. J Gene Med. 2005; 7:739–748. [PubMed: 15685706]
46. Behr JP. Photohydrolysis of DNA by polyaminobenzenediazonium salts. J Chem Soc Chem Commun. 1989:101–103.
47. Koltover I, Salditt T, Safinya CR. Phase diagram, stability, and overcharging of lamellar cationic lipid-DNA self-assembled complexes. Biophys J. 1999; 77:915–924. [PubMed: 10423436]
48. Salditt T, Koltover I, Rädler JO, Safinya CR. Two-dimensional smectic ordering of linear DNA chains in self-assembled DNA-cationic liposome mixtures. Phys Rev Lett. 1997; 79:2582–2585.
49. Salditt T, Koltover I, Rädler JO, Safinya CR. Self-assembled DNA–cationic-lipid complexes: Two-dimensional smectic ordering, correlations, and interactions. Phys Rev E: Stat Phys, Plasmas, Fluids, Relat Interdiscip Top. 1998; 58:889–904.
50. Koltover I, Wagner K, Safinya C. DNA condensation in two dimensions. Proc Natl Acad Sci U S A. 2000; 97:14046–14051. [PubMed: 11121015]
51. Bloomfield V. Condensation of DNA by multivalent cations: considerations on mechanism. Biopolymers. 1991; 31:1471–1481. [PubMed: 1814499]
52. Bloomfield V. DNA condensation. Curr Opin Struct Biol. 1996; 6:334–341. [PubMed: 8804837]
53. Bloomfield V. DNA condensation by multivalent cations. Biopolymers. 1997; 44:269–282. [PubMed: 9591479]
54. Pelta J, Livolant F, Sikorav J. DNA aggregation induced by polyamines and cobalthexamine. J Biol Chem. 1996; 271:5656–5662. [PubMed: 8621429]
55. Luzzati V, Husson F. The structure of the liquid-crystalline phases of lipid-water systems. J Cell Biol. 1962; 12:207–219. [PubMed: 14467542]

56. Luzzati V, Reiss-Husson F, Rivas E, Gulik-Krzywicki T. Structure and Polymorphism in Lipid-Water Systems, and Their Possible Biological Implications. Ann N Y Acad Sci. 1966; 137:409–413. [PubMed: 5229807]
57. Tardieu A, Luzzati V, Reman FC. Structure and polymorphism of the hydrocarbon chains of lipids: a study of lecithin-water phases. J Mol Biol. 1973; 75:711–733. [PubMed: 4738730]
58. Luzzati, V. X-ray Diffraction Studies of Lipid-Water Systems. In: Chapman, D., editor. Biological membranes: physical fact and function. Vol. 1. Academic Press; London, New York: 1968. p. 71-123.
59. Bouxsein NF, Leal Cl, McAllister CS, Ewert KK, Li Y, Samuel CE, Safinya CR. Two-Dimensional Packing of Short DNA with Nonpairing Overhangs in Cationic Liposome–DNA Complexes: From Onsager Nematics to Columnar Nematics with Finite-Length Columns. J Am Chem Soc. 2011; 133:7585–7595. [PubMed: 21520947]
60. Bouxsein N, McAllister C, Ewert K, Samuel C, Safinya C. Structure and Gene Silencing Activities of Monovalent and Pentavalent Cationic Lipid Vectors Complexed with siRNA. Biochemistry. 2007; 46:4785–4792. [PubMed: 17391006]
61. Subramanian M, Holopainen JM, Paukku T, Eriksson O, Huhtaniemi I, Kinnunen PK. Characterisation of Three Novel Cationic Lipids as Liposomal Complexes with DNA. Biochim Biophys Acta. 2000; 1466:289–305. [PubMed: 10825450]
62. Doe C, Jang HS, Kim TH, Kline SR, Choi SM. Thermally Switchable One- and Two-Dimensional Arrays of Single-Walled Carbon Nanotubes in a Polymeric System. J Am Chem Soc. 2009; 131:16568–16572. [PubMed: 19902979]
63. Bain CD, Troughton EB, Tao YT, Evall J, Whitesides GM, Nuzzo RG. Formation of Monolayer Films by the Spontaneous Assembly of Organic Thiols from Solution onto Gold. J Am Chem Soc. 1988; 111:321–335.
64. Prime KL, Whitesides GM. Self-assembled Organic Monolayers: Model Systems for Studying Adsorption of Proteins at Surfaces. Science. 1991; 252:1164–1167.

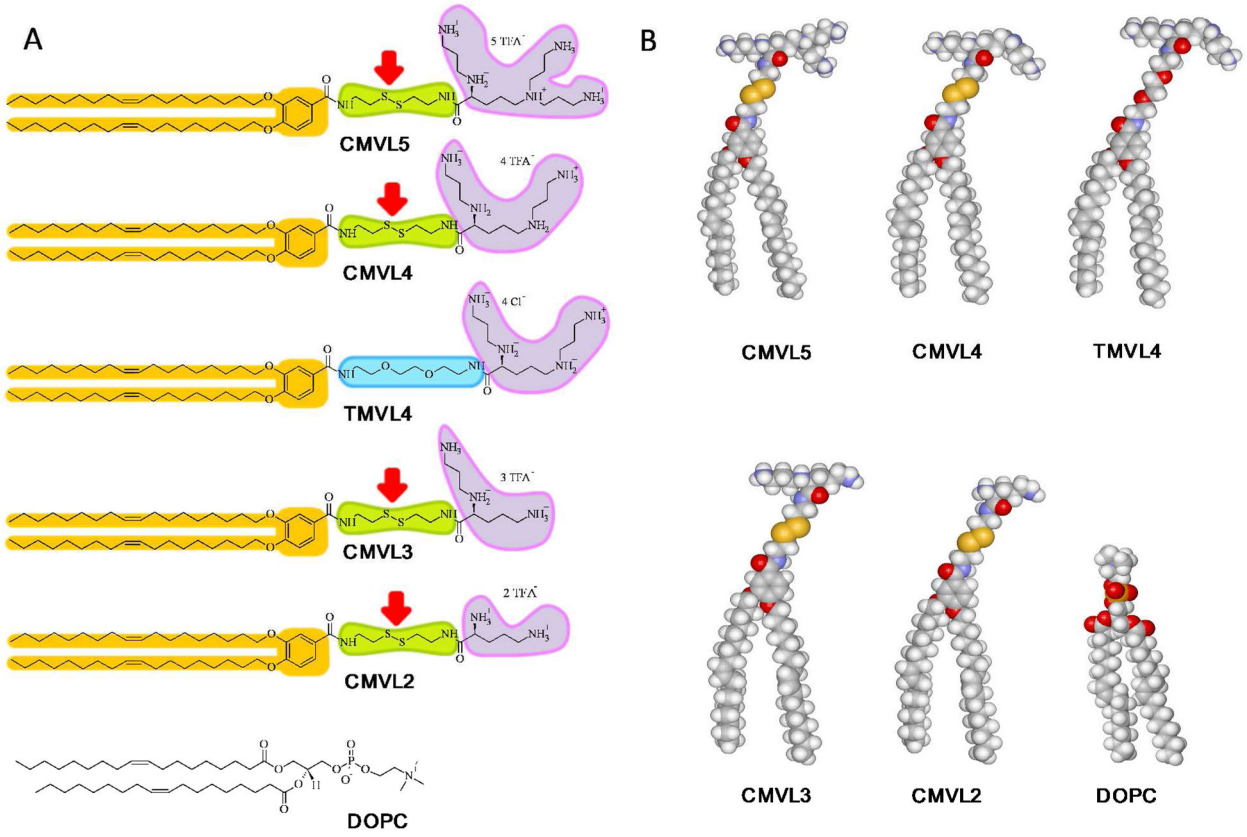

Figure 1.

(A) The chemical structures of the CMVLs, TMVL4, and DOPC. CMVL headgroups are shown fully protonated. The alkyl tails are identical for all molecules. The reducible disulfide bond in the linker of the CMVLs is indicated by a red arrow. (B) Molecular models of the CMVLs, TMVL4, and DOPC.

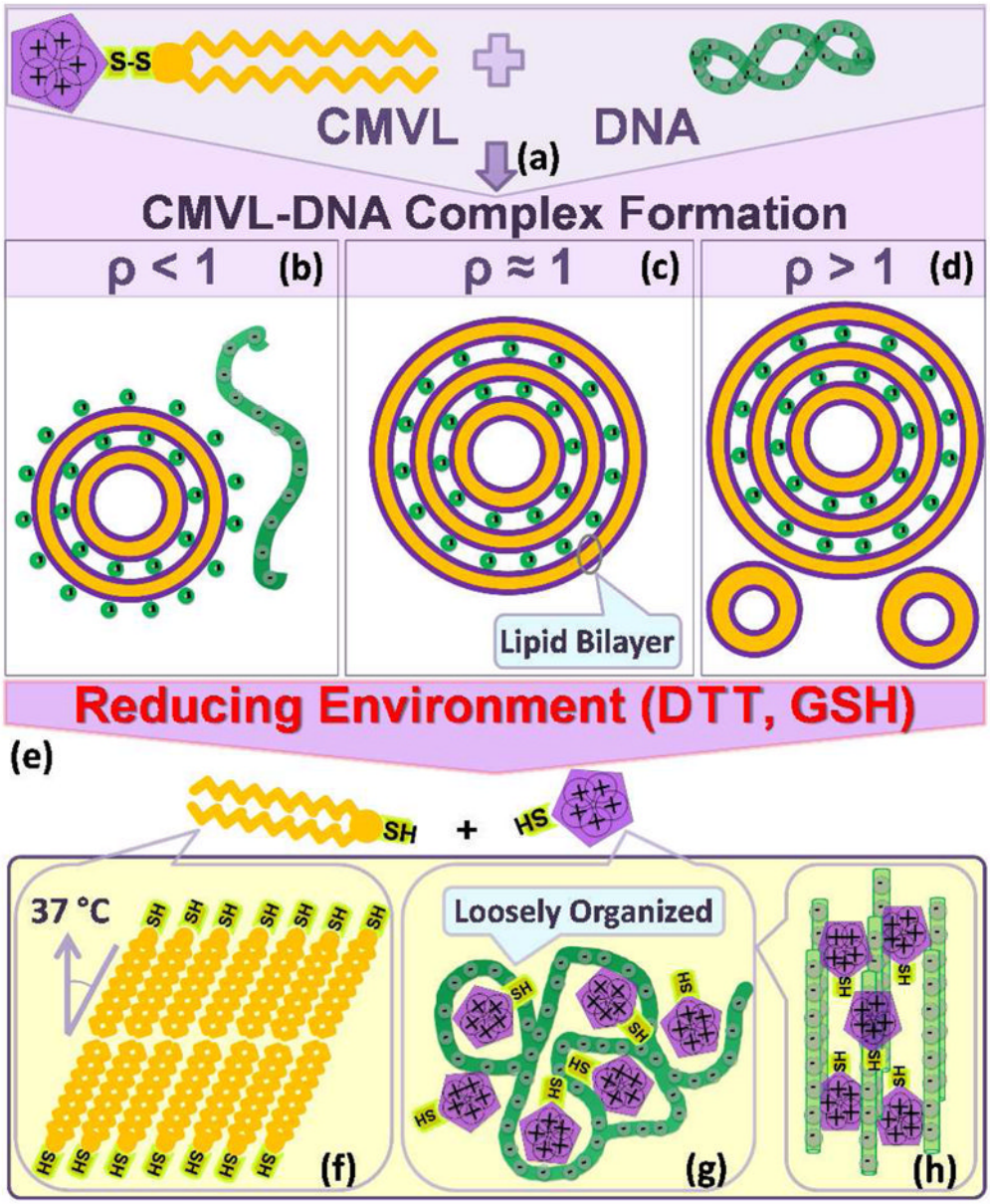

Figure 2.

Schematic depiction of the formation of CMVL–DNA complexes and the evolution of their structure in response to a reducing environment. Mixing aqueous solutions of DNA and cationic liposomes containing the CMVL leads to spontaneous formation of CMVL–DNA complexes with a multilamellar structure (a). The entropy gained from the release of the small counterions of the DNA and the CMVL liposomes is the main driving force for complex formation. At CMVL/DNA charge ratios (ρ) below one, anionic complexes (b) form, which coexist with free DNA at small ρ. At the isoelectric point (ρ = 1), where the charges on the DNA and the CMVL match, neutral complexes are formed (c). For values of ρ near the isoelectric point, all DNA and liposomes are incorporated into the complexes, resulting in charged complexes.[47] At large ρ (excess CMVL) positively charged complexes coexist with CMVL liposomes (d). Reducing agents cleave the disulfide linker between the headgroup and the hydrophobic tails of the CMVL (e), resulting in disassembly of the

lamellar complexes. The cleaved parts of the CMVLs become the building blocks for new phases that form as a function of headgroup charge, time and temperature. The cationic headgroups condense the released DNA into a “loosely organized” phase (g) with a characteristic broad SAXS correlation profile. This phase can evolve into a phase of tightly condensed hexagonal bundles of DNA for CMVLs with high headgroup charge (h). In addition, incubation at 37 °C for 24 hours (after cleavage with the reducing agent DTT) induces self-assembly of the cleaved hydrocarbon into chain-ordered lamellar phases with tilted chains (f).

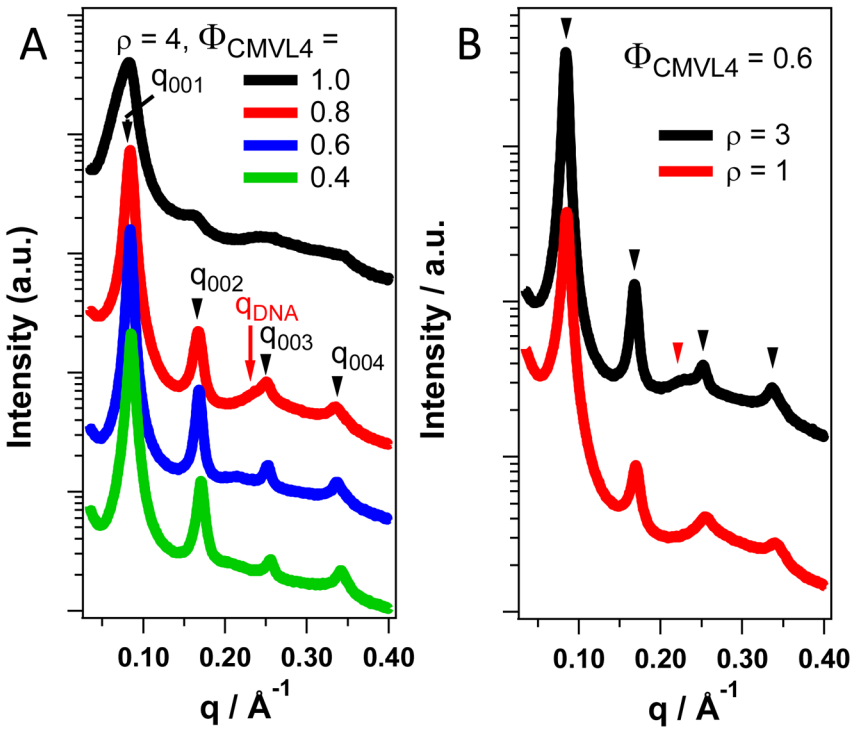

Figure 3.

Synchrotron SAXS profiles of CMVL4/DOPC–DNA complexes at varied Φ_{CMVL4} and ρ in a nonreducing environment. (A) Data for complexes at varied Φ_{CMVL4} (1.0 to 0.4) at ρ = 4. Black arrows point to the characteristic peaks resulting from the lamellar structure (L_α^C) on the curve for Φ_{CMVL4} = 0.8. The red arrow points to the DNA correlation peak. All complexes are in the lamellar phase. (B) The L_α^C phase is also observed at ρ = 3 and ρ = 1, as shown here for complexes with Φ_{CMVL4} = 0.6 at room temperature. Black arrowheads point to the q_{00n} peaks resulting from the lamellar structure and the red arrowhead points to the DNA correlation peak (d_{DNA} = 27.7 Å).

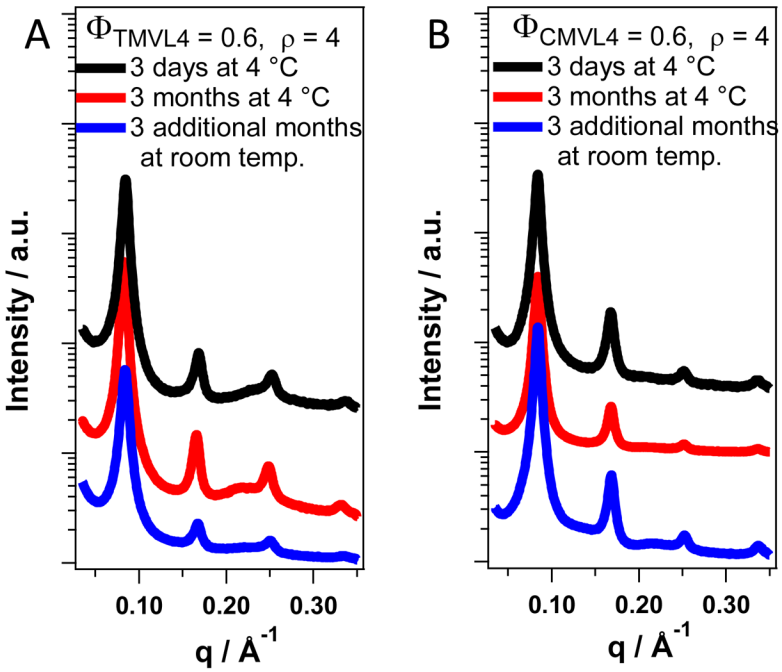

Figure 4.

SAXS profiles of DNA complexes prepared from CMVL4 and TMVL4 in nonreducing medium continue to show the characteristic pattern of the lamellar phase after 3 and 6 months incubation at room temperature. The only changes are slight shifts in the lamellar peak positions and increases in the intensity of the DNA–DNA which can be attributed to equilibration of the samples.

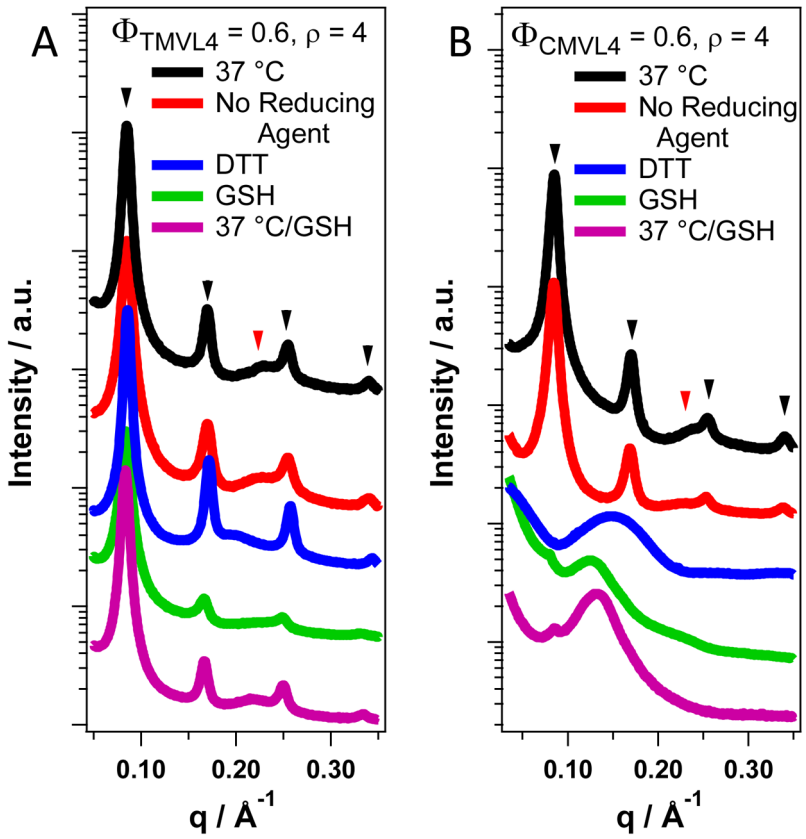

Figure 5.

SAXS data for complexes prepared from TMVL4 and CMVL4 (ρ = 4, Φ_{DOPC} = 0.4) incubated at different temperatures and with reducing agents. Black arrowheads mark peaks resulting from the lamellar ordering; red arrowheads mark the DNA correlation peak. (A) The scattering patterns of TMVL4-based complexes do not change upon addition of either reducing agent (DTT and GSH) or change in temperature, i.e., the complexes remain lamellar. Incubation at 37 °C was for 8 hours. The sample containing GSH was incubated an additional 5 months at 4 °C (magenta curve). (B) The scattering patterns of CMVL4-based complexes are strongly affected by the addition of reducing agents but not by incubation at physiological temperature without reducing agent. The peaks characteristic for the lamellar structure disappear completely (DTT) or almost completely (GSH) and a new broad peak at $q = 0.15$ Å^{-1} (DTT) or $q \approx 0.13$ Å^{-1} (GSH) appears. The sample incubated with GSH at 4 °C for one month also shows a faint broad peak at $q = 0.22$ Å^{-1} which is absent in the sample incubated at 37 °C. Incubation at 37 °C was for 8 hours in all cases.

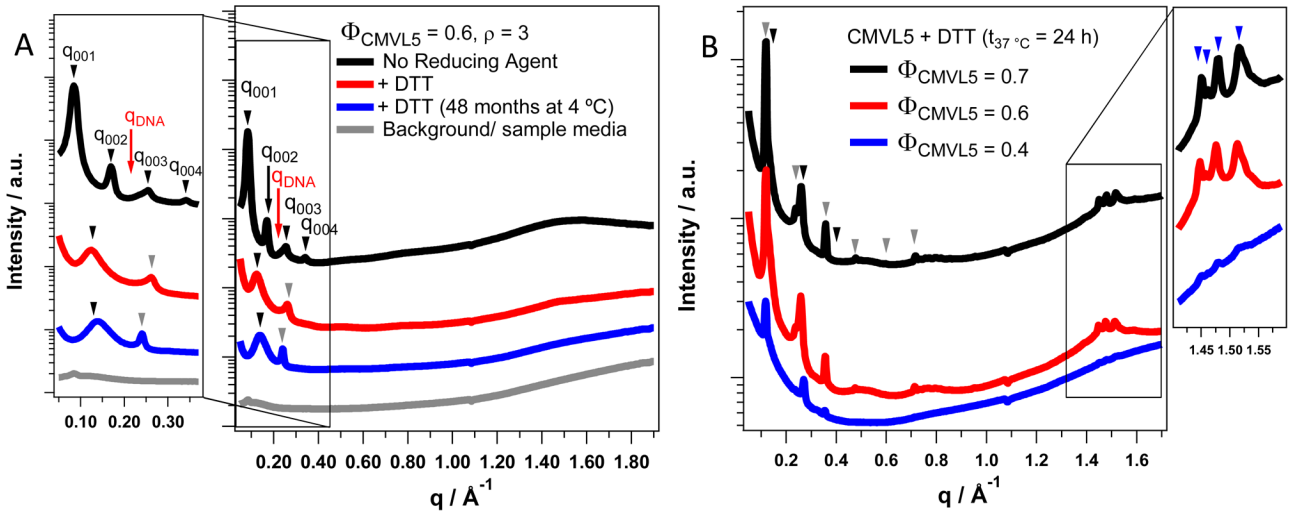

Figure 6.

Small- and wide-angle X-ray scattering data for CMVL5-containing complexes (ρ = 3) incubated with and without the reducing agent DTT at 4 °C and 37 °C. The wide-angle diffraction data provides information on the structures formed by the lipid tails. (A) The scattering pattern of complexes $^{at}\ \Phi_{CMVL5} = 0.6$ without reducing agent at room temperature (black curve, top) shows the characteristic peaks of the lamellar $L_\alpha{}^C$ phase (black arrows mark q_{00n}, red arrow marks q_{DNA}), with $d_{DNA} = 27.3$ Å. Upon addition of DTT at room temperature (red curve, middle), these peaks disappear and new peaks arise: a broad peak at $q \approx 0.125$ Å^{-1} and a sharp peak $q = 0.26$ Å^{-1}. After 48 months incubation at 4 °C (blue curve, bottom), a similar sample (same composition, prepared independently) shows a broad peak at $q \approx 0.13$ Å^{-1} and a sharp peak at $q = 0.24$ Å^{-1}. Also shown is the background scattering from the sample medium without complexes. The broad shallow peak between $q = 1.3$ and 1.7 Å^{-1} observed for all the above samples indicates that the hydrophobic tails are in the chain-melted state without long-range order. (B) The scattering patterns of complexes at varied Φ_{CMVL5} that were incubated with DTT at 37 °C for 24 h show numerous sharp peaks at both small and larger q. The small angle peaks index to two coexisting lamellar phases (black and gray arrowheads) while the wide-angle peaks (at $q = 1.45$ Å^{-1}, 1.46 Å^{-1}, 1.48 Å^{-1}, and 1.51 Å^{-1}) show that these new phases contain chain-ordered lipid tails.

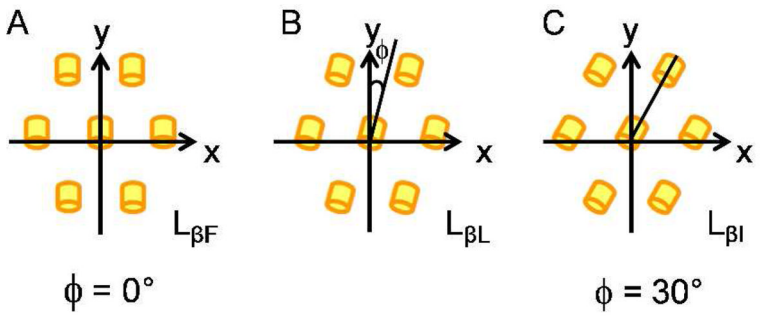

Figure 7.

Schematic illustration of the relative orientation of the tilted lipid tails in the three phases comprised by the $L_{\beta'}$ phase. Yellow cylinders represent the in-plane projections of the lipid tails. The phases differ in the azimuthal angle (φ) as shown. For the $L_{\beta F}$ and the $L_{\beta I}$ phase with $\varphi = 0°$ (A) and $\varphi = 30°$ (C), respectively, there is a reflection symmetry about the tilt direction. In $L_{\beta L}$ phase (B) the reflection symmetry about the tilt direction is broken. Adapted from Smith et al.[42]